Dynamic correlations and heterogeneity in the primary and secondary relaxations of a model molecular liquid

D. Fragiadakis and C. M. Roland
Naval Research Laboratory, Chemistry Division, Code 6120, Washington, DC 20375-5342, USA
(Received 6 February 2014; published 6 May 2014)

Molecular dynamics simulations were carried out on a series of Lennard-Jones binary mixtures of rigid, asymmetric, dumbbell-shaped molecules. Below an onset temperature, the rotational and translational dynamics split into the slow structural α relaxation and a higher-frequency Johari-Goldstein β relaxation. Both processes are dynamically heterogeneous, having broad distributions of relaxation times. However, only the α relaxation shows strong dynamic correlations; correlations at the β time scale are weak, in particular for molecules having shorter bonds. Despite the close connection between the two processes, we find no correlation between the α and β relaxation times of individual molecules; that is, a molecule exhibiting slow β motion does not necessarily undergo slow α dynamics and likewise for fast molecules. However, the single-molecule α relaxation times do correlate with both the α and β relaxation strengths.

DOI: 10.1103/PhysRevE.89.052304 PACS number(s): 64.70.pm, 61.20.Ja, 33.15.Vb

I. INTRODUCTION

The dynamics of glass-forming liquids is complex, with correlated motions taking place over various time scales that can differ by many orders of magnitude. In addition to the primary α relaxation, associated with structural relaxation and the glass transition, supercooled liquids and glasses show faster secondary motions. Unique among these is the Johari-Goldstein (JG) β relaxation, ubiquitous in glass-forming materials including molecular liquids and polymers [1,2], ionic liquids [3], metallic glasses [4,5], and plastic crystals [6]. The JG relaxation involves all atoms in the molecule (or polymer repeat unit) and appears even in liquids of completely rigid molecules. Unlike intramolecular secondary relaxations, the JG process is intimately related to structural relaxation and the glass transition: Several well-documented correlations exist between the two modes of motion [7], and at high temperatures the JG and α relaxations evolve into a single process. Based on these relationships, a series of criteria have been proposed to distinguish the genuine JG process from secondary processes of intramolecular origin [8,9]. In the glassy state the suppression of structural relaxation usually leaves the JG process as the dominant mode of motion, whereby it may affect properties such as the mechanical response of polymers [10,11] and the stability of biomolecules [12] and amorphous pharmaceuticals [13,14]. Several decades after its discovery, the molecular motions underlying the JG process and the latter's coupling to the α relaxation remain unclear.

Except at very high temperatures, the α process in liquids is non-Arrhenius and nonexponential. It has been well established experimentally [15] and by molecular dynamics simulations [16] that this behavior stems from dynamic heterogeneity, i.e., the coexistence of molecules with substantially different relaxation times. This heterogeneity is spatially correlated, being organized into fast and slow regions with a characteristic size that increases on cooling or compressing, concomitant with a dramatic slowing down of the α relaxation [17–19]. Connections can be made between dynamic heterogeneity and cooperativity of the α process; the latter refers to the fact that relaxation of a molecule requires rearrangement of other molecules.

Dynamic heterogeneity, dynamic correlations, and intermolecular cooperativity are inherent to the many-body interactions governing molecular motions in dense, viscous liquids, but notwithstanding their putative interrelations, the underlying concepts are not the same. Dynamic heterogeneity refers to the coexistence of molecules or regions with different relaxation times, but this dispersity does not imply anything about the spatial arrangement, or lack thereof, of molecules with similar mobilities [20]. The latter is described by dynamic correlations, i.e., spatial correlations among molecules with similar mobilities to form clusters. Dynamic correlations are usually quantified using the four-point susceptibility χ_4 or associated quantities [19]. Dynamic heterogeneity and correlations usually arise from cooperativity, molecular motions exerting reciprocal influences. However, this is not necessarily the case. For example, one can imagine a local noncooperative relaxation which shows dynamic heterogeneity and dynamic correlations-—faster and slower regions over a given length scale—due to inhomogeneity unrelated to the relaxation process, such as spatial fluctuations in the molecular packing or local composition of a blend. Conversely, a process such as the relaxation of the end-to-end vector in long polymer chains is cooperative (except in dilute solution, chains cannot relax independently of one another due to physical entanglements), but it can be dynamically homogeneous due to averaging over the chain end-to-end length scale. In the case of the α relaxation, the length scale of dynamic correlations has been invoked as a measure of a cooperativity length, or at least its upper bound [18]. However, there are reasons to question such a direct relationship between the two quantities [21], with cooperativity more accurately described as stringlike simultaneous rearrangements [22], particles undergoing simultaneous correlated hops [23], or from point-to-set correlation lengths [24,25].

It is well established that the Johari-Goldstein β process is dynamically heterogeneous [26]. But does it also exhibit dynamic correlations and cooperativity? Dynamic correlations at the β time scale and in the region of the α-β crossover need more study, and the degree of cooperativity involved in the JG relaxation remains an open question. In Johari's "islands of mobility" interpretation, the JG process is due to

noncooperative, small-amplitude rearrangements of molecules located in loosely packed regions [27]. However, Johari and Goldstein in their original papers describing the process ascribed it to rearrangements of "at least one, but probably several molecules" [1], which admits the possibility of cooperativity. The high activation energy and activation entropy of the JG process in the glassy state have been interpreted as indicative of some degree of cooperativity [28,29]; to distinguish this type of cooperativity from that exhibited by the α process, the former has been termed "locally coordinative" [30]. By similar arguments, it has been concluded that the range of barrier heights for the JG relaxation overlaps, but may be somewhat lower than, those for the α relaxation [31]. Random first-order theory [32] ascribes the JG process to rearrangements of stringlike clusters of molecules. Some degree of intermolecular cooperativity is implied indirectly by NMR measurements of binary mixtures [33] and organic phosphate glasses [34], and also can be inferred from the effect of immobilized particles on the high-frequency mechanical response of a simulated Lennard-Jones system [35].

In this work we use molecular dynamics simulations to investigate dynamic heterogeneity of the β process, to determine its relation to heterogeneity of the α relaxation and whether the former is also associated with dynamic correlations. We simulate a family of rigid, asymmetric, dumbell-shaped molecules studied previously [9,36]; these comprise one of the simplest molecular models that captures the characteristics observed experimentally for the JG process. The simulated system shows β dynamics that by its definition of involving all parts of the molecule is a JG relaxation. This process shows many of the correlations experimentally observed: merging with the α process at high temperatures, a change in behavior when traversing the glass transition temperature T_g, temporal separation from the α relaxation that correlates with the breadth of the α dispersion, and sensitivity to both pressure and physical aging. These characteristics suggest that this process has the same physical origin as the JG relaxation in real materials, so that conclusions drawn from our simulations can be extended to the latter.

II. METHODS

Simulations were carried out using the HOOMD simulation package [37,38]. The systems studied are binary mixtures (4000:1000, labeled AB and CD) of rigid, asymmetric, diatomic molecules. Atoms belonging to different molecules interact through the Lennard-Jones potential,

$$U_{ij}(r) = 4\varepsilon_{ij}\left[\left(\frac{\sigma_{ij}}{r}\right)^{12} - \left(\frac{\sigma_{ij}}{r}\right)^{6}\right], \qquad (1)$$

where r is the distance between particles, and i and j refer to the particle types A, B, C, and D. The energy and length parameters ε_{ij} and σ_{ij} are based on the Kob-Andersen (KA) liquid, a binary mixture not prone to crystallization [39]. The procedure was as follows (noting that alternative choices of ε_{ij} and σ_{ij} give qualitatively similar results): The energy parameters ε_{ij} are those of the KA liquid; i.e., $\varepsilon_{\rm AA} = \varepsilon_{\rm AB} = \varepsilon_{\rm BB} = 1.0$, $\varepsilon_{\rm CC} = \varepsilon_{\rm CD} = \varepsilon_{\rm DD} = 0.5$, and $\varepsilon_{\rm AC} = \varepsilon_{\rm AD} = \varepsilon_{\rm BC} = \varepsilon_{\rm BD} = 1.5$. To set σ_{ij} we use the original KA parameters for the larger A and C particles, while the B and D particles are 50% smaller than A and C, respectively. Therefore, $\sigma_{\rm AA} = 1$, $\sigma_{\rm CC} = 0.88$, $\sigma_{\rm BB} = 0.5$, and $\sigma_{\rm DD} = 0.44$. For the particle interactions we take $\sigma_{ij} = S_{ij}(\sigma_{ii}+\sigma_{jj})$, where $S_{ij} = 0.5$ (additive interaction) when the particles belong to the same type of molecule (i, j = AB, CD), and $S_{ij} = 0.4255$ when the particles belong to different types, the latter chosen to give the KA value for $\sigma_{\rm AC} = 0.8$. All atoms have a mass of $m = 1$. The bond lengths A-B and C-D were fixed using rigid-body dynamics [40]. All quantities are expressed in dimensionless Lennard-Jones units: length $\sigma_{\rm AA}$, temperature $\varepsilon_{\rm AA}/k_{\rm B}$, and time $(m\sigma_{\rm AA}^2/\varepsilon_{\rm AA})^{1/2}$. Unless specified otherwise, we calculate the rotational and translational dynamics of the AB molecules (the behavior of the CD molecules is qualitatively the same).

A family of liquids with bond lengths $d = 0.45$, 0.5, and 0.6 were simulated. Simulations were carried out in an *NVT* ensemble. Densities were chosen to maintain a constant packing fraction of approximately 0.63; this results in a similar pressure range ($\sim 0 < P < 10$) for all molecules studied. The densities were $\rho = 1.3$, 1.25, and 1.175, for the respective bond lengths above. Simulations at constant pressure give qualitatively identical results [36]. The time step was $\Delta t = 0.005$. Data were collected at each temperature after an equilibration run several times longer than the structural relaxation time. At low temperatures structural relaxation is extremely slow, whereby the translational and orientational correlation functions do not decay to zero over the duration of the simulation; i.e., the system is out of equilibrium. For these conditions we increased the equilibration time, until neither significant drift in the volume nor aging of the translational and rotational correlation functions was observed; the residual motion of the molecules at these temperatures takes place within a nonequilibrium, but essentially static structure.

The glass transition occurs in the simulations when the α relaxation time is much longer than the total (equilibration and production) simulation time at a given temperature, which is about $t_{\rm max} \sim 10^6$. This is about seven orders of magnitude slower than the vibrational relaxation times, which for a real liquid corresponds to time scales in the 10^{-5} s range, much shorter than the $\sim$100 s for the usual experimental glass transition.

III. RESULTS AND DISCUSSION

A. Dynamic correlations

The dynamics of these same diatomic molecules has been discussed previously in Refs. [9,36]. From the instantaneous value of the self-intermediate scattering function,

$$f_s(q,t) = \frac{1}{N}\sum_{j=1}^{N} \exp\{i\mathbf{q}\cdot[\mathbf{r}_j(t) - \mathbf{r}_j(0)]\}, \qquad (2)$$

where $\mathbf{r}_j(t)$ is the position of the center of mass of the jth molecule, we calculate the average value $F_s(k,t) = \langle f_s(k,t)\rangle$, used to study the translational dynamics of the molecules, and the four-point susceptibility,

$$\chi_4(q,t) = N\left[\left\langle f_s^2(q,t)\right\rangle - \langle f_s(q,t)^2\rangle\right], \qquad (3)$$

which describes dynamic correlations. We take $q = q_{\rm max}$, the position of the first maximum in the center-of-mass radial

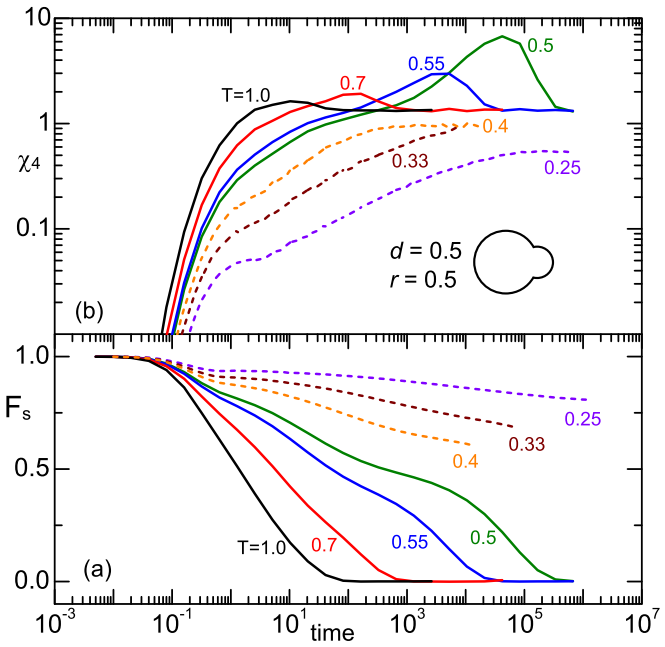

FIG. 1. (Color online) (a) Center-of-mass self-intermediate scattering function and (b) associated four-point susceptibility (upper panel) for the molecule with bond length $d = 0.5$, at the temperatures shown.

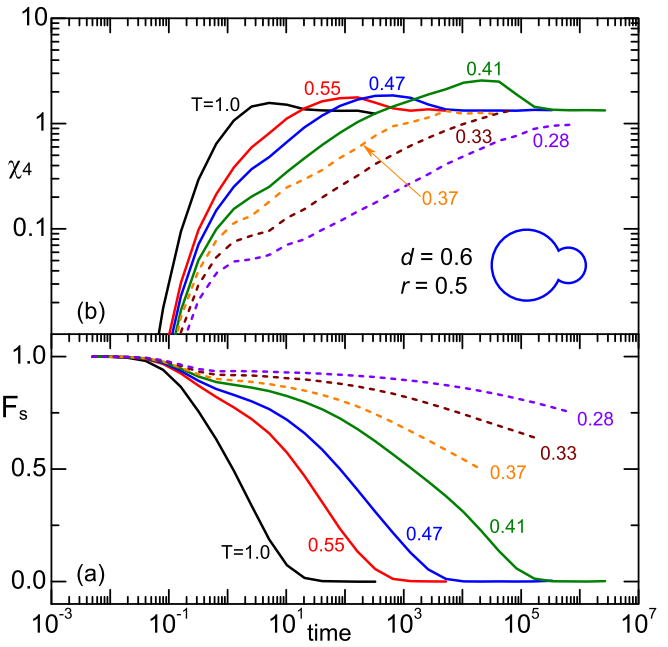

FIG. 2. (Color online) (a) Center-of-mass self-intermediate scattering function and (b) associated four-point susceptibility for the molecule with bond length $d = 0.6$, at the temperatures shown.

distribution function. The absolute values of the four-point susceptibility depend on the thermodynamic ensemble (*NVT* herein); however, the shape of the function is similar for different ensembles, describing essentially the same physics [41].

The self-intermediate scattering function is shown in the lower panels of Figs. 1 and 2 for molecules with bond lengths $d = 0.5$ and 0.6. Translational dynamics shows very similar behavior to the rotational dynamics discussed in Refs. [9,36]. At short times there is a small decrease of $F_s(q,t)$ corresponding to oscillations within the cage formed by neighboring particles, at a temperature-independent time scale $\tau_{\rm vib} \sim 0.1$. At high temperatures F_s then decays to zero via a single step. Below an onset temperature $T_{\rm on}$ the relaxation occurs in two steps: a shorter time β and a longer time α process. The latter appears as a long-time tail, which grows in strength with decreasing temperature at the expense of the β intensity. At even lower temperatures, the α relaxation time is much larger than the simulation time; the system is in a nonequilibrium glassy state. Nevertheless, F_s relaxes significantly; the magnitude of the nonzero plateau value increases with decreasing temperature.

The four-point susceptibility $\chi_4(t)$ is shown in the upper panels of Figs. 1 and 2. The general behavior of χ_4 is similar to that for other atomic and molecular glass-forming liquids. There is a single maximum, $N_c = \max \chi_4(t)$, quantifying the number of dynamically correlated molecules. This N_c and the time scale of the maximum, τ_4, are plotted in Fig. 3 as a function of temperature for a series of molecules with different bond lengths. At high temperatures τ_4 is close to τ_β, which corresponds to the structural relaxation time τ_α, as N_c has a value close to unity. At the onset temperature, where the

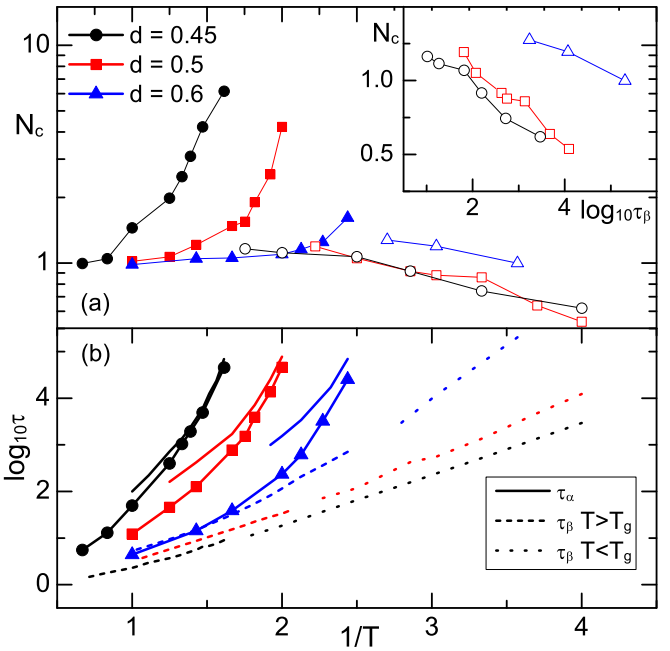

FIG. 3. (Color online) (a) Number of dynamically correlated molecules N_c, determined as the maximum value of $\chi_4(t)$, as a function of temperature for molecules with bond length 0.45, 0.5, and 0.6. Filled symbols represent the α relaxation and open symbols the β process. (Note that above the onset temperature there is only one relaxation that is continuous with τ_β.) (b) Corresponding times τ_4 (points), α relaxation times (solid lines), and β relaxation times (dashes above T_g, dots below T_g). Inset in upper panel: N_c as a function of $\log \tau_\beta$ in the glassy state.

translational and rotational relaxation functions both split into distinct α and β processes, N_c for the α relaxation begins to increase with decreasing temperature, and τ_4 approaches τ_α as the α intensity increases at the expense of the β relaxation strength.

At relatively low temperatures for which the two processes are clearly separated, there is only a weak shoulder in χ_4 at the time scale of the β process. This means that unlike the α process, the β dynamics is only weakly spatially correlated. In the glassy state, where the α process time scale is much longer than the simulation time, χ_4 has no clear maximum but only a shoulder around τ_β with maximum values of N_c on the order of unity and decreasing slightly on cooling. (The values of N_c less than unity in Fig. 3 are artifacts from omission of a proportionality constant in its relation to max $\chi_4(t)$ [42].)

There is a systematic effect of molecular shape on the behavior of N_c. With increasing bond length, the primary relaxation becomes less correlated; i.e., N_c is smaller for a given state point or value of τ_α. Conversely, the weak dynamic correlations at the β process time scale become larger for a given τ_β with increasing bond length (inset of Fig. 3), both in the liquid and glassy states, consistent with the increase in β activation energy.

B. Relationship between α and β heterogeneity

We now investigate the relationship between heterogeneity of the α and β processes. We ask, for example, whether molecules with a fast α process also have a fast β process. This requires a way to distinguish fast and slow molecules. To do this we define a single-molecule rotational correlation function, in an analogous way to those calculated from experimental data on single-molecule relaxation [43]. To capture dynamic heterogeneity, we average only over a finite time interval $[0, t_{\rm ave}]$:

$$C_1^{(i)}(t; t_{\rm ave}) = \langle \cos\theta^{(i)}(t_0) \cos\theta^{(i)}(t_0 + t) \rangle_{t_0 \in [0, t_{\rm ave}]}. \quad (4)$$

The value of $t_{\rm ave}$ requires some consideration. If must be long enough to yield an adequate signal-to-noise ratio, but short compared to the lifetime of the heterogeneity or to the time scale $\tau_{\rm het}$ over which mobility exchange takes place and dynamic heterogeneity dissipates. When $\tau_{\rm ave} \gg \tau_{\rm het}$, ergodicity of the system implies that the single-molecule $C_1^{(i)}$ will become equal to the average correlation function for the ensemble,

$$C_1(t) = \frac{1}{N} \sum_{j=1}^{N} C_1^{(j)}(t). \quad (5)$$

Unfortunately, it is not always possible to find a suitable averaging time scale; however, for sufficiently wide separation of the relaxation times, $\tau_\alpha \gg \tau_\beta$, we found that $t_{\rm ave} = \tau_\alpha/2$ gives good results. In the following we present data only for the molecule with $d = 0.5$ at the lowest temperature in the liquid state ($T = 0.5$), where the separation of the two processes was largest. Representative single-molecule correlation functions are shown in Fig. 4. To extract single-molecule relaxation times and strengths, we fit the portion of the $C_1^{(i)}$ curves from $t = 1$ (longer than vibrational time scale) to $t = t_{\rm ave}$ with the sum of

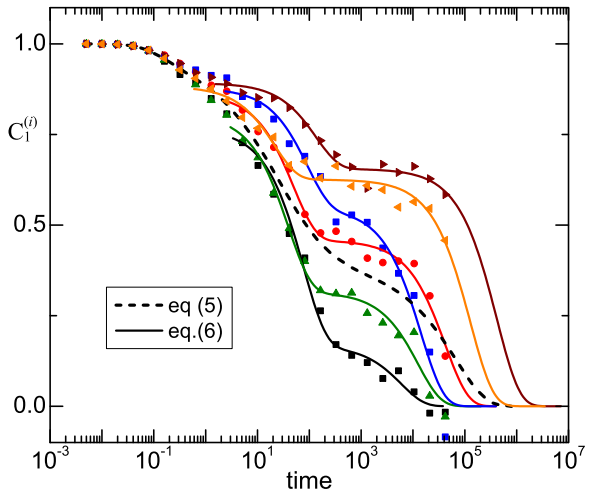

FIG. 4. (Color online) Single-molecule orientational correlation functions of six representative molecules for the liquid with $d = 0.5$, at $T = 0.5$ as defined in Eq. (4). Solid lines are fits to Eq. (6); dashed line is the ensemble average dynamics.

two exponentials,

$$C_1^{(i)}(t) = \Delta C_\alpha^{(i)} \exp\left(-\frac{t}{\tau_\alpha^{(i)}}\right) + \Delta C_\beta^{(i)} \exp\left(-\frac{t}{\tau_\beta^{(i)}}\right). \quad (6)$$

This is not intended to provide an accurate description of the single-molecule correlation function; Eq. (6) is employed to obtain an estimate of the relaxation times and relative intensities for the two processes. The noise in the data does not allow any firm conclusion about whether the individual relaxation functions are exponential, although the data are compatible with that assumption. From the fits we obtain single-molecule values of the relaxation times and intensities for every molecule.

We find broad distributions of τ_α and τ_β, indicating strong dynamic heterogeneity at the time scales of both processes. The dynamics also exhibits heterogeneity in a different way: The distributions of the intensities of the two processes are also broad. We can look for correlations between these distributions. The distributions $G_\alpha(\tau_\alpha)$ and $G_\beta(\tau_\beta)$ of the two relaxation times and the correlation between them are shown in Fig. 5 in the format used by Böhmer *et al.* in Ref. [44]. No correlation is found; the two relaxation times are independent. On the other hand, the relaxation strengths of the two processes are well correlated. Since the relaxation function is normalized from 0 to 1, the latter correlation is trivial, and follows from the fact that the vibrational amplitude $\Delta C_{\rm vib}^{(i)} = 1 - \Delta C_\beta^{(i)} - \Delta C_\alpha^{(i)}$ is small and does not vary much among molecules. We also examine the correlation between relaxation strength and relaxation time for each process (Fig. 6). These are moderately correlated ($R = 0.63$) for the α process: Molecules with a more intense α process also tend to have longer τ_α. For the JG process, the β relaxation strengths and τ_β are uncorrelated, as found previously for the glassy state [36].

We can visualize these correlations in a different way by defining dynamically distinguishable subsets of molecules and observing the dynamics of those subsets at various time scales. We define four subsets, labeled slow-α, fast-α,

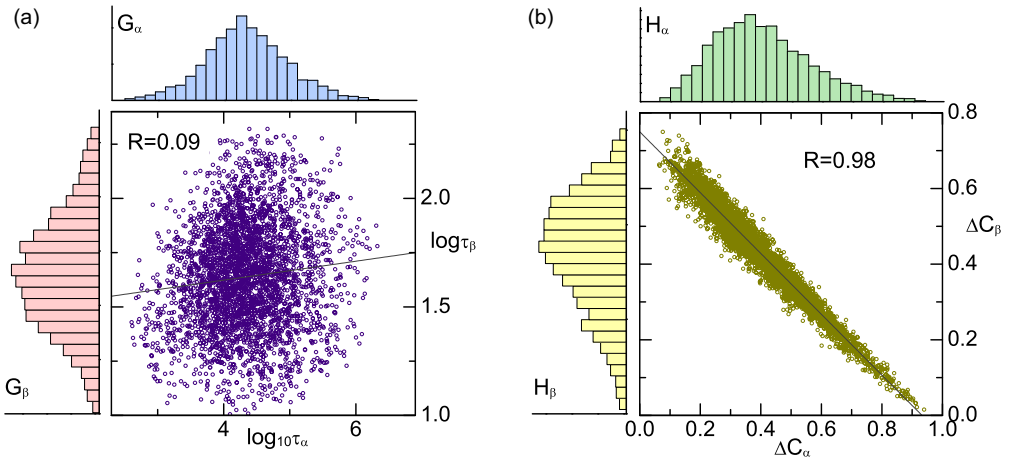

FIG. 5. (Color online) (a) Correlation of single-molecule relaxation times τ_β vs τ_α and (b) relaxation strengths ΔC_β vs ΔC_α for the liquid with $d = 0.5$ at $T = 0.5$. Also shown are the respective distributions of relaxation times and strengths.

slow-β, and fast-β, as the 5% of AB molecules having the longest and shortest τ_α and τ_β, respectively. In Fig. 7 we show the imaginary part χ'' of the dynamic susceptibility,

$$\chi(\omega) = \chi'(\omega) + i\chi''(\omega) = 1 + i\omega \int_0^\infty dt e^{i\omega t} F_s(\mathbf{q},t), \quad (7)$$

as a function of frequency (for an averaging time of 2.5×10^5) for the four subsets. Also displayed is the average dynamics for all molecules. The slow-α subset has significantly stronger α and weaker β, which shows the coupling between τ_α and the relaxation strengths; however, the β relaxation time and shape are the same as for the average dynamics. As expected, the α relaxation of the slow-α and fast-α subsets is also narrower than the ensemble average α process (stretching exponents $= 0.86$, ~ 1, and 0.73 for the slow-α, fast-α, and ensemble average, respectively). On the other hand, slow-β and fast-β molecules have the same α relaxation strength and α relaxation time as the average value, indicating decoupling of the β relaxation dynamics of individual molecules from the mean α relaxation behavior.

The presence of strong heterogeneity but only very weak dynamic correlations at the β time scale means there can be no well-defined regions with fast- or slow-β dynamics. Rather, the relaxation time is randomly distributed spatially, with no characteristic length scale. Since the α process is strongly dynamically correlated, this implies a lack of correlation between the α and β distributions of relaxation times, as indeed is found. This is because if there were a strong correlation between these distributions, then any dynamic correlations and spatially resolved regions with distinct dynamics would be similar at the two time scales. Note that an analogous disconnect between fast, local motion and slow, cooperative dynamics is observed in colloidal suspensions [45]. Ion conduction exhibits similar behavior: At short times there are fast and slow diffusing species, with dynamic exchange occurring at longer times [46].

It is surprising that despite the plethora of correlations between the *average* α and β relaxation times, the single-molecule τ_α and τ_β for a given state point do not correlate. For example, the widths of the two relaxation peaks, related to the breadth of the distributions of relaxation times, are not correlated for different materials, as seen in the data collected

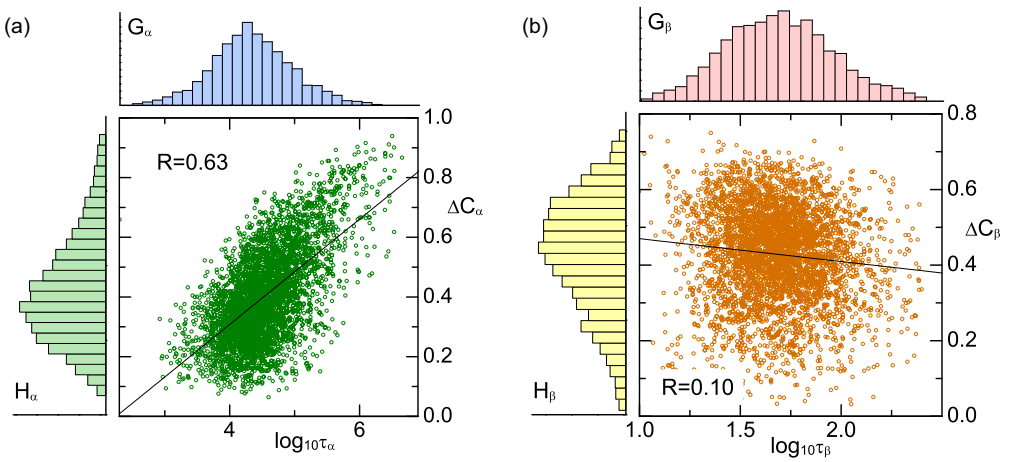

FIG. 6. (Color online) Correlation of single-molecule relaxation intensity and relaxation time for the (a) α and (b) β processes. Also shown are the respective distributions of relaxation times and strengths.

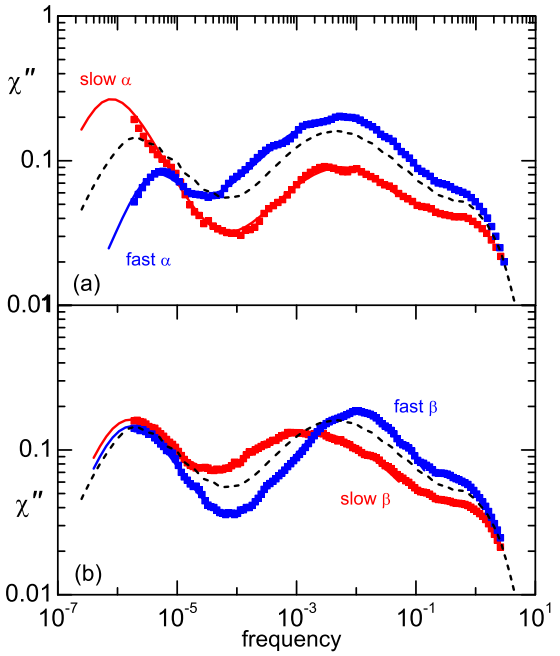

FIG. 7. (Color online) First-order rotational susceptibility as a function of frequency, for the molecule with $d = 0.5$ at $T = 0.5$ for the sets of 5% molecules with (a) fastest and slowest α process and (b) fastest and slowest β process. Dashed lines are the average system dynamics. Solid lines are fits to a sum of a Cole-Cole term for the β process and the Fourier transform of a stretched exponential term for the α process.

in Ref. [47]. Also among different materials, the breadth of the distribution of α relaxation times exhibits no correlation to dynamic heterogeneity [48].

Experimentally it is challenging to determine directly whether there is a correlation between the two distributions. Böhmer and co-workers, using a nuclear magnetic resonance (NMR) method simultaneously sensitive to dynamics at both time scales, found evidence consistent with a correlation of the two distributions [44,49,50]. At first this seems incompatible with the present simulation results. However, we also find heterogeneity in the relative strengths of the α and β processes, which was not considered in the interpretation of the NMR measurements. However, it is important to note that there is a correlation of the strengths with the α relaxation time: molecules with a stronger β and weaker α process have a faster α process. NMR is not able to probe directly the correlations of τ_α and τ_β. Instead, essentially a subset of molecules is selected that is able to relax significantly at a time scale $t_{\rm filt}$ comparable to but smaller than τ_β. These molecules are interpreted as a subset with a faster β process, and the dynamics of this subset, followed at longer times, is found to have a shorter τ_α. We carried out an analogous procedure using the simulation data: Figure 8 shows the dynamics of a subset of molecules corresponding to the 10% with the smallest value of $c_1^{(j)}(t_{\rm filt})$, for $\tau_{\rm filt} \simeq 0.1\tau_\beta$. These indeed have a faster β process, although they also have stronger β and weaker α intensities. This effect on the relaxation strengths is what leads, based on the correlations of Figs. 5 and 6, to a shorter τ_α, notwithstanding

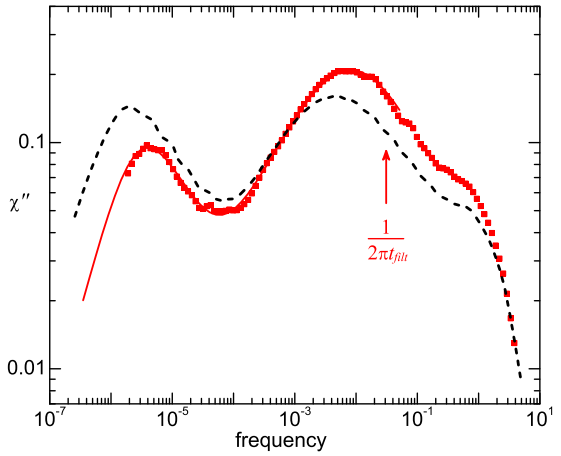

FIG. 8. (Color online) Imaginary part of the first-order rotational susceptibility as a function of frequency, for the molecule with $d = 0.5$ at $T = 0.5$ for the 10% of molecules having the smallest value of rotational correlation function at a time scale $t_{\rm filt} \simeq 0.1\tau_\beta$ (points) and for all molecules (dashed line). Solid lines are fits to a sum of a Cole-Cole term for the β process and the Fourier transform of a stretched exponential term for the α process.

the lack of correlation between the distributions of τ_α and τ_β *per se*.

C. Lifetime of heterogeneity

From the dynamics of the subsets described previously (slow-α, fast-α, slow-β, and fast-β), we can determine the time scale over which the heterogeneity of the α and β processes dissipates. Increasing the averaging time, the dynamics of all

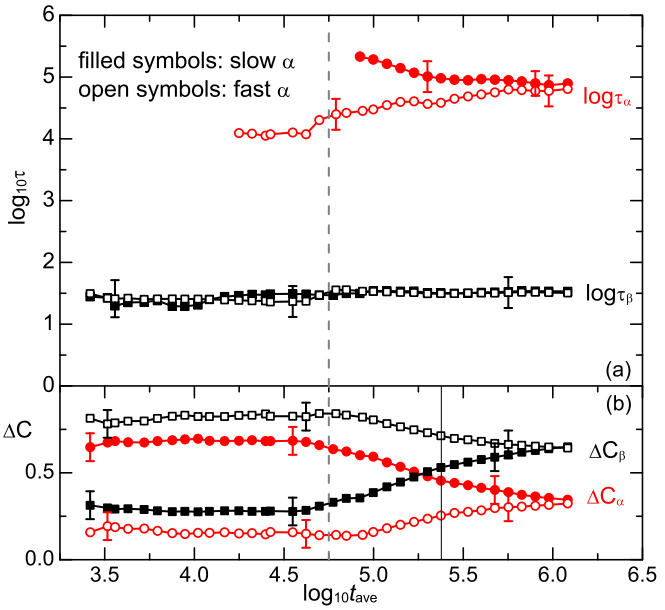

FIG. 9. (Color online) Averaging time dependence of the α and β (a) relaxation times and (b) relaxation strengths for the sets of 10% molecules with fastest (open symbols) and slowest (filled symbols) α process. Also shown are τ_α (vertical dashed line) and $\tau_{\rm het}$ (vertical solid line).

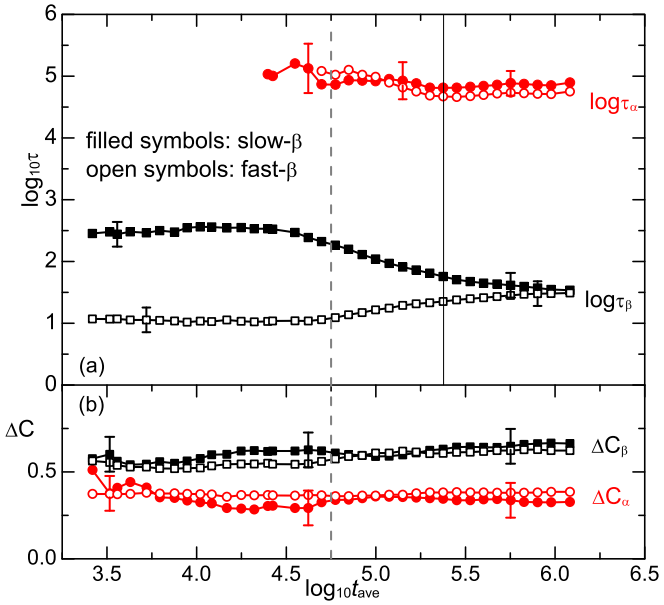

FIG. 10. (Color online) Averaging time dependence of the α and β (a) relaxation times and (b) relaxation strengths for the sets of 5% molecules with fastest (open symbols) and slowest (filled symbols) β process. Also shown are τ_α (vertical dashed line) and $\tau_{\rm het}$ (vertical solid line).

four subsets gradually revert to the average dynamics, since the system is ergodic. Fitting the relaxation functions with the sum of a time-domain Cole-Cole function and a stretched exponential for the respective β and α processes, we obtain the relaxation times and intensities as a function of averaging times shown in Figs. 9 and 10. With increasing averaging time, as the heterogeneity of the α relaxation dissipates (slow-α and fast-α subsets), the relaxation strengths and τ_α approach their average values. For the heterogeneity of the β process (slow-β and fast-β subsets), we follow τ_β as a function of averaging time. We define the lifetime of heterogeneity $\tau_{\rm het}$ as the averaging time at which the relaxation strengths recover $1/e$ of the difference between the initial (unaveraged) and final (ensemble averaged) value. A single heterogeneity lifetime is obtained for both the β and α relaxations, in agreement with deuteron NMR results on molecular liquids [26]. This time scale is somewhat longer than the α relaxation time, $\tau_{\rm het} \simeq (4.0 \pm 0.5)\tau_\alpha$. In the literature a wide range of values has been reported from experimental studies, with the results depending on the precise definition of $\tau_{\rm het}$ and the experimental technique. In a recent survey of the literature, generally $\tau_{\rm het} \simeq 3\tau_\alpha$ with no significant temperature dependence [15], consistent with our result.

IV. SUMMARY

Molecular dynamics (MD) simulations of rigid, asymmetric, dumbell-shaped molecules were used to investigate the Johari-Goldstein process. The simulated molecules exhibit the properties commonly observed for the JG relaxation in real materials, and given their lack of intramolecular degrees of freedom, their β process complies with the definition of the JG process as involving all atoms in a molecule. We examine herein two aspects of the complex dynamics of supercooled liquids—dynamic correlations and dynamic heterogeneity. At lower temperatures, the number of dynamically correlated molecules approaches values of 10 on time scales commensurate with τ_α, while the dynamic correlations for the JG are weak. At high temperatures for which the JG and α relaxations have merged, N_c attains the value unity, reflecting loss of all correlation. Both processes, however, are markedly heterogeneous, with broad distributions of single-molecule relaxation times. Interestingly, there is no correlation between the dynamic heterogeneity of the two relaxations; molecules undergoing fast JG motion have no tendency to evolve into a subsequent rapid α process, nor vice versa. This result is at odds with recent conclusions from NMR measurements [44,49,50]. The discrepancy is due to the correlation of the relaxation strengths with τ_α, whereby molecules associated with faster β processes have larger intensities. It is the latter that underlies the faster α dynamics. The lifetime of dynamic heterogeneities is longer than the α relaxation time by about a factor of 4, in accord with experiments.

In summary, the JG relaxation has connections to the α process, but these do not unambiguously support the idea that the JG serves as the precursor to structural relaxation. In particular, the respective magnitudes of $\tau_{\rm JG}$ and τ_α for individual molecules show no evidence that the former "become" the latter. The manner in which short-time, local dynamics evolves into low-frequency relaxation processes is more complex, and understanding this is obviously essential to a first-principles solution to the long-standing problem of the glass transition.

ACKNOWLEDGMENT

This work was supported by the Office of Naval Research.

[1] G. P. Johari and M. Goldstein, J. Chem. Phys. **53**, 2372 (1970).
[2] K. Pathmanathan and G. P. Johari, J. Polym. Sci., Part B: Polym. Phys. **25**, 379 (1987).
[3] G. Jarosz, M. Mierzwa, J. Zioło, M. Paluch, H. Shirota, and K. L. Ngai, J. Phys. Chem. B **115**, 12709 (2011).
[4] H.-B. Yu, W.-H. Wang, and K. Samwer, Mater. Today **16**, 183 (2013).
[5] H. B. Yu, K. Samwer, Y. Wu, and W. H. Wang, Phys. Rev. Lett. **109**, 095508 (2012).
[6] R. Brand, P. Lunkenheimer, and A. Loidl, J. Chem. Phys. **116**, 10386 (2002); Th. Bauer, M. Köhler, P. Lunkenheimer, A. Loidl, and C. A. Angell, *ibid.* **133**, 144509 (2010).
[7] K. L. Ngai, J. Chem. Phys. **109**, 6982 (1998).
[8] K. L. Ngai and M. Paluch, J. Chem. Phys. **120**, 857 (2004).

[9] D. Fragiadakis and C. M. Roland, Phys. Rev. E **88**, 042307 (2013).
[10] L. P. Chen, A. F. Yee, and E. J. Moskala, Macromolecules **32**, 5944 (1999).
[11] L. Monnerie, F. Laupretre, and J. L. Halary, Adv. Polym. Sci. **187**, 35 (2005); L. Monnerie, J. L. Halary, and H.-H. Kausch, *ibid.* **187**, 215 (2005).
[12] M. T. Cicerone and J. F. Douglas, Soft Matter **8**, 2983 (2012).
[13] S. Bhattacharya and R. Suryanarayanan, J. Pharm. Sci. **98**, 2935 (2009).
[14] Z. Wojnarowska, C. M. Roland, K. Kolodziejczyk, A. Swiety-Pospiech, K. Grzybowska, and M. Paluch, J. Phys. Chem. Lett. **3**, 1238 (2012).
[15] R. Richert, N. Israeloff, C. Alba-Simionesco, F. Ladieu, D. L'Hôte, in *Dynamical Heterogeneities in Glasses, Colloids, and Granular Media*, edited by L. Berthier, G. Biroli, J.-P. Bouchaud, L. Cipeletti, and W. van Saarloos (Oxford University Press, Oxford, 2011), p. 152.
[16] P. Harrowell, in *Dynamical Heterogeneities in Glasses, Colloids, and Granular Media*, edited by L. Berthier, G. Biroli, J.-P. Bouchaud, L. Cipeletti, and W. van Saarloos (Oxford University Press, Oxford, 2011), p. 229.
[17] H. Sillescu, J. Non-Cryst. Solids **243**, 81 (1999).
[18] M. D. Ediger, Annu. Rev. Phys. Chem. **51**, 99 (2000).
[19] L. Berthier, G. Biroli, J.-P. Bouchaud, R. L. Jack, in *Dynamical Heterogeneities in Glasses, Colloids, and Granular Media*, edited by L. Berthier, G. Biroli, J.-P. Bouchaud, L. Cipeletti, and W. van Saarloos (Oxford University Press, Oxford, 2011), p. 68.
[20] H. Sillescu, R. Böhmer, G. Diezemann, and G. Hinze, J. Non-Cryst. Solids **307**, 16 (2002).
[21] C. Dalle-Ferrier, C. Thibierge, C. Alba-Simionesco, L. Berthier, G. Biroli, J.-P. Bouchaud, F. Ladieu, D. L'Hôte, and G. Tarjus, Phys. Rev. E **76**, 041510 (2007).
[22] C. Donati, J. F. Douglas, W. Kob, S. J. Plimpton, P. H. Poole, and S. C. Glotzer, Phys. Rev. Lett. **80**, 2338 (1998).
[23] A. Smessaert and J. Rottler, Phys. Rev. E **88**, 022314 (2013).
[24] L. Berthier and W. Kob, Phys. Rev. E **85**, 011102 (2012).
[25] A. Cavagna, T. S. Grigera, and P. Verrocchio, J. Chem. Phys. **136**, 204502 (2012).
[26] R. Böhmer, G. Hinze, T. Jörg, F. Qi, and H. Sillescu, J. Phys.: Condens. Matter **12**, A383 (2000).
[27] G. P. Johari, J. Chem. Phys. **58**, 1766 (1973).
[28] H. W. Starkweather, Macromolecules **14**, 1277 (1981); **21**, 1798 (1988).
[29] J. F. Mano and S. Lanceros-Méndez, J. Appl. Phys. **89**, 1844 (2001).
[30] F. Garwe, A. Schönhals, H. Lockwenz, M. Beiner, K. Schröter, and E. Donth, Macromolecules **29**, 247 (1996).
[31] M. Goldstein, J. Chem. Phys. **132**, 041104 (2010).
[32] J. D. Stevenson and P. G. Wolynes, Nat. Phys. **6**, 62 (2010).
[33] D. Bock, R. Kahlau, B. Micko, B. Pötzschner, G. J. Schneider, and E. A. Rössler, J. Chem. Phys. **139**, 064508 (2013).
[34] R. Kahlau, T. Dörfler, and E. A. Rössler, J. Chem. Phys. **139**, 134504 (2013).
[35] Y. Cohen, S. Karmakar, I. Procaccia, and K. Samwer, Europhys. Lett. **100**, 36003 (2012).
[36] D. Fragiadakis and C. M. Roland, Phys. Rev. E **86**, 020501(R) (2012).
[37] HOOMD Web page: http://codeblue.umich.edu/hoomd-blue.
[38] J. A. Anderson, C. D. Lorenz, and A. Travesset, J. Comput. Phys. **227**, 5342 (2008).
[39] W. Kob and H. C. Andersen, Phys. Rev. E **48**, 4364 (1993).
[40] T. D. Nguyen, C. L. Phillips, J. A. Anderson, and S. C. Glotzer, Comput. Phys. Commun. **182**, 2307 (2011).
[41] L. Berthier, G. Biroli, J.-P. Bouchaud, W. Kob, K. Miyazaki, and D. R. Reichman, J. Chem. Phys. **126**, 184503 (2007).
[42] L. Berthier and G. Bioli, Rev. Mod. Phys. **83**, 587 (2011).
[43] D. Bingemann, R. M. Allen, and S. W. Olesen, J. Chem. Phys. **134**, 024513 (2011).
[44] B. Geil, G. Diezemann, and R. Böhmer, Phys. Rev. E **74**, 041504 (2006).
[45] E. R. Weeks, J. C. Crocker, A. C. Levitt, A. Schofield, and D. A. Weitz, Science **287**, 627 (2000).
[46] J. Habasaki and K. L. Ngai, J. Non-Cryst. Solids **352**, 5170 (2006).
[47] L.-M. Wang and R. Richert, Phys. Rev. B **76**, 064201 (2007).
[48] C. M. Roland, D. Fragiadakis, D. Coslovich, S. Capaccioli, and K. L. Ngai, J. Chem. Phys. **133**, 124507 (2010).
[49] R. Böhmer, G. Diezemann, B. Geil, G. Hinze, A. Nowaczyk, and M. Winterlich, Phys. Rev. Lett. **97**, 135701 (2006).
[50] A. Nowaczyk, B. Geil, G. Hinze, and R. Böhmer, Phys. Rev. E **74**, 041505 (2006).